JOURNAL OF GEOPHYSICAL RESEARCH, VOL. 115, C04022, doi:10.1029/2009JC005448, 2010

A unified deep-to-shallow water wave-breaking probability parameterization

Jean-François Filipot,[1] Fabrice Ardhuin,[1] and Alexander V. Babanin[2]

Received 18 April 2009; revised 10 November 2009; accepted 20 November 2009; published 27 April 2010.

[1] Breaking probabilities and breaking wave height distributions (BWHDs) in deep, intermediate, and shallow water depth are compared, and a generic parameterization is proposed to represent the observed variability of breaking parameters as a function of the nondimensional water depth. In intermediate and deep water, where waves of different scales may have markedly different breaking probabilities, a BWHD as a function of wave frequency is proposed and validated with intermediate-depth and deep water observational data. The current study focuses on waves with frequencies between 0.55 and 3.45 times the peak frequency f_p. For the dominant frequency, the integration of the frequency-dependent BWHD provides a breaking probability that reproduces the known threshold-type behavior of the breaking probability for dominant waves. In shallow water, the present breaking statistics parameterization is consistent with other independent formulations validated by shallow water-breaking observations.

Citation: Filipot, J.-F., F. Ardhuin, and A. V. Babanin (2010), A unified deep-to-shallow water wave-breaking probability parameterization, *J. Geophys. Res.*, *115*, C04022, doi:10.1029/2009JC005448.

1. Introduction

[2] Breaking of surface gravity waves plays a major role in many oceanographic and air-sea interaction processes. Wave breaking is the main energy sink term for the wave field [e.g., *WISE Group*, 2007] and strongly affects the remote sensing of ocean properties [e.g., *Reul and Chapron*, 2003]. There is, hence, a need to model wave-breaking statistics in order to estimate parameters such as the white-cap coverage, the surface renewal rate, or the average foam thickness. The evolution of individual waves toward breaking is not yet fully understood [e.g., *Banner and Peregrine*, 1993], and no general consensus exists either on a method for predicting the statistics of breaking random waves, or on the amount of energy lost during breaking. In numerical wave models, wave-breaking dissipation in deep and shallow water is parameterized by two different source terms.

[3] In deep water, the most widely used dissipation terms are based on generic forms proposed by *Komen et al.* [1984] that have no link to wave-breaking observations. Such parameterizations are contradicted by experimental evidence that the breaking probabilities of dominant deep water and finite-depth random waves are controlled by a threshold in the average steepness of the dominant waves as shown by *Banner et al.* [2000] and *Babanin et al.* [2001] and theoretically by *Papadimitrakis* [2006]. Also, the dissipation at small scales appears to depend on the spectrum at larger scales. This "cumulative effect" is discussed by *Babanin and Young* [2005], *Young and Babanin* [2006], *Babanin et al.* [2007b] and is likely connected with the variation with wave age of the transition frequency between the f^{-4} and f^{-5} asymptotes, observed by *Long and Resio* [2007]. It may be caused by the breaking of long waves and the modulation of the short waves. A proper model for the cumulative effect probably requires the parameterization of the breaking probability of the long waves [e.g., *Ardhuin et al.*, 2009]. Besides, all parameterizations of the kind proposed by *Komen et al.* [1984] are unrealistically sensitive to the presence of long-period swells [e.g., *van Vledder and Hurdle*, 2002; *Ardhuin et al.*, 2007].

[4] In shallow water, wave-breaking dissipation is usually parameterized following *Battjes and Janssen* [1978] or *Thornton and Guza* [1983]. However, wave breaking in deep, intermediate and shallow water share many common features, and there is no obvious physical reason to formulate completely differently the deep and shallow water breaking. This usual practice generally fails as wind waves propagate in shallow water and both parameterizations may be active at the same time. Indeed, waves start breaking when the orbital velocity at the crest u_c approaches or reaches the wave phase speed C, i.e., $\alpha \approx 1$ with $\alpha = u_c/C$, which defines the highest possible periodic wave. In the present study, we rely on that criterion in order to parameterize the breaking statistics.

[5] As shown, for example, by *Wu and Nepf* [2002], irregular waves start breaking when $\alpha \approx 1$. Other works have reported smaller values, by up to 20% [*Stansell and MacFarlane*, 2002]. Because periodic waves of heights lower than the highest waves have a larger energy [*Cokelet*, 1977], these

[1] Service Hydrographique et Océanographique de la Marine, Brest, France.
[2] Faculty of Engineering and Industrial Sciences, Swinburne University of Technology, Melbourne, Victoria, Australia.

0148-0227/10/2009JC005448

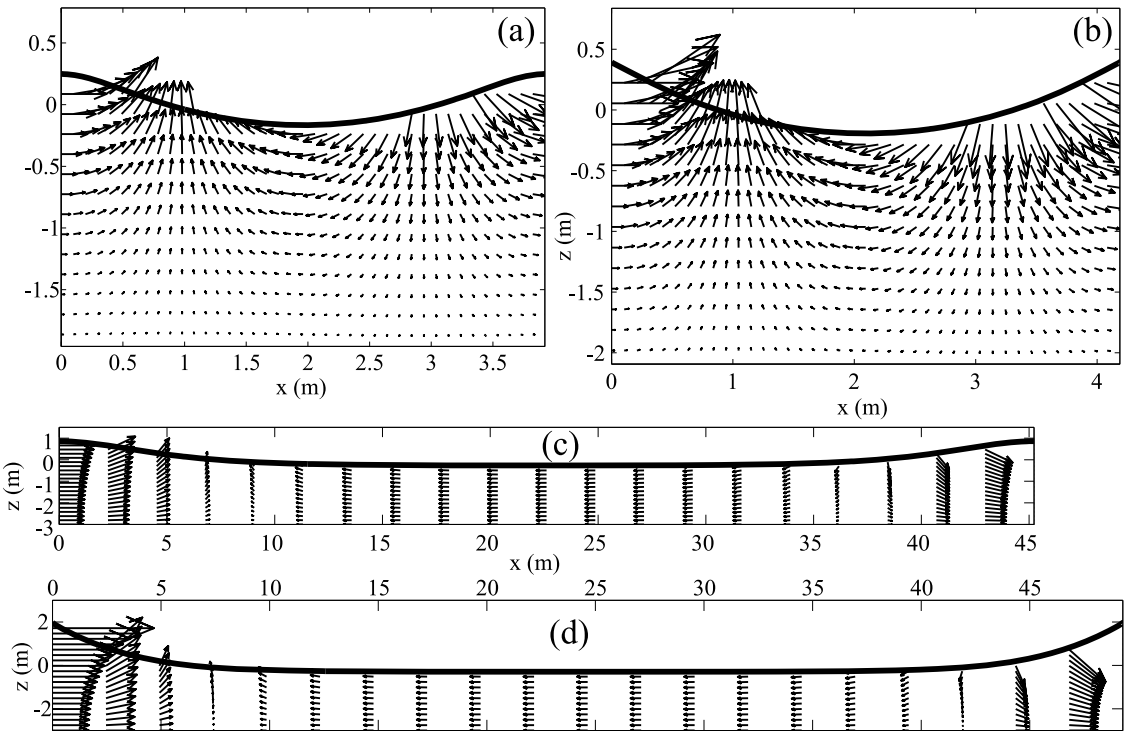

Figure 1. Wave profiles computed with *Dalrymple*'s [1974] method to the 60th order. The arrows represent orbital velocities. (a and b) Waves with a period $T = 1.5$ s ($kD \simeq 5$), corresponding thus to deep water waves. (c and d) Shallow water waves ($T = 8$ s, $kD \simeq 0.45$). The waves in Figures 1a and 1c are moderately nonlinear ($u_c/C \simeq 0.3$), whereas those in Figures 1b and 1d are nearly breaking ($u_c/C \simeq 0.97$).

almost highest waves are unstable [*Tanaka*, 1985] and may break before reaching the condition $\alpha = 1$ (see *Banner and Peregrine* [1993] for a review). Besides, the numerical investigation of steep waves also shows that u_c varies dramatically as waves approach their highest possible form, typically increasing by 30% when the wave height only increases by 5%, as illustrated by Figure 1. As a result, a very accurate estimation of the orbital velocity is not necessary to get a decent approximation for the height of the incipient breaking waves.

[6] For one-dimensional, periodic, irrotational waves over a flat bottom, *Miche* [1944a] shows that the breaking criterion $\alpha = 1$ can be conveniently converted into the condition

$$\frac{kH_{\max}}{\beta_{\max}\tanh(kD)} = 1, \tag{1}$$

where D is the water depth, k the wave number, $H_{\max}$ the maximal wave height and $\beta_{\max} = 0.88$, a value also consistent with the results of *Longuet-Higgins* [1975]. This condition has inspired numerous shallow water studies where it appears under the form $H_{\max} = \tilde{\gamma}D$, with $\tilde{\gamma}$ a nondimensional parameter.

[7] As we attempt to reconcile deep and shallow water approaches for random waves, it is important to emphasize that investigations of deep water waves have long tried to reveal a deterministic breaking threshold for random waves, but only a threshold for the spectral density has been established [*Banner et al.*, 2000], this is thus a probabilistic threshold. Any individual wave is given a breaking probability that smoothly varies from zero to one as a function of its steepness.

[8] Such a probabilistic approach has also been used in shallow water by *Thornton and Guza* [1983] who expressed the breaking wave height distribution (BWHD) in terms of $H/\tilde{\gamma}D$ with $\tilde{\gamma} = H_{rms}/D$. From their data, *Thornton and Guza* [1983] reported that $\tilde{\gamma} = 0.42$. Although a similar parameter $\tilde{\gamma}$ is used, this probabilistic approach to breaking is fundamentally different from the earlier work by *Battjes and Janssen* [1978] who used a deterministic threshold for breaking: in that model, any wave of height smaller than $\tilde{\gamma}D$ does not break, and all other waves are limited to a height of $\tilde{\gamma}D$ and are breaking. The observed BWHD contains breaking waves at different stages of the breaking process, as a result, it is natural to expect a broad distribution of the BWHD.

[9] Investigations by *Battjes and Stive* [1985] and *Ruessink et al.* [2003], without breaking probability observations but based on the wave energy balance of *Battjes and Janssen* [1978], suggest that $\tilde{\gamma}$ should be a function of the nondimensional water depth $\overline{k}D$ where $\overline{k}$ is a representative wave number. This approach has been extended to deep water by *Chawla and Kirby* [2002] who used the nonlinearity parameter initially introduced by [*Miche*, 1944a]

$$\beta = kH/\tanh(kD). \tag{2}$$

It is interesting to note that, for linear monochromatic waves, $\beta = 2u_c/C$.

[10] Such a generalization of shallow water parameterizations, however, does not give any information on the possible

variation of the breaking probabilities as a function of frequency, which may be needed to clearly separate swells from wind seas, a problem that has not been considered in shallow water, where it may be irrelevant. Recently, using a joint distribution of wave frequencies and amplitudes and a deterministic breaking threshold, *Papadimitrakis* [2006] derived an analytical expression for the breaking probability in deep water as a function of frequency. Independent analyses by *Banner et al.* [2000] have related observed breaking probabilities for dominant waves, using the surface elevation filtered around the peak frequency f_p, to a steepness parameter derived from a part of the spectrum. This approach was repeated by *Banner et al.* [2002] for higher frequencies. These breaking probabilities show a variation as a function of the relative frequency f/f_p, but later they have been interpreted as an evidence for a cumulative effect. Namely, the breaking probability of waves may be augmented by the presence of longer waves [*Babanin et al.*, 2007b].

[11] Our intention is, thus, to reconcile all these observations and provide a practical parameterization of breaking probabilities in terms of the wave spectrum. This work is the first building block of a universal spectral dissipation parameterization that is intended for the numerical wave models, in which, so far, wave-breaking dissipation in deep and shallow water has been parameterized by two different source terms. In section 2 we review the analysis of *Miche* [1944b] for regular, irrotational waves over a flat bottom in order to provide a theoretical basis for the interpretation of wave-breaking observations in various water depths and define a semiempirical BWHD. This parameterization is applied in section 3 to random waves in shallow, intermediate and deep water. Conclusions follow in section 4.

2. Periodic and Irrotational Waves in One Dimension With a Flat Bottom

[12] Extending the work of Stokes, *Miche* [1944b] analyzed waves of finite amplitude in nondimensional depths $0.56 < kD < 2.2$, where D is the mean water depth and k is the wavenumber, providing an analytical approximate solution for the stream function and velocity potential of periodic symmetric incipient breaking waves of permanent form. These waves exhibit a 120 sharp angle at their crest, due to the equality of the wave orbital velocity at the crest u_c with the phase speed C. Thanks to Froude scaling of the gravity waves, the shape and kinematics of such incipient breaking waves is only a function of kD. One may thus parameterize this family of waves and the general set of two-dimensional periodic waves can be further defined by the two parameters kD and $0 < u_c/C < 1$. Here we use numerical solutions for nearly breaking waves, obtained with the stream function wave theory of *Dean* [1965] and *Dalrymple* [1974] applied to 80th order. The wave profile and kinematics were computed using dimensional values, with a water depth $D = 3$ m, and the acceleration of gravity $g = 9.81\text{m s}^{-2}$. The wave period T was varied from 1.8 to 35 s, and for each wave period the wave height is progressively increased until $\alpha = u_c/C$ is at least 0.97. The numerical accuracy is constrained by an error function such that the root-mean-square (RMS) deviation of the surface pressure from zero is less than 1 mm for $T < 20$ s and less than 1 cm for larger values of T. Therefore this analysis improves the accuracy and extends the range investigated by Miche to $0.06 < kD < 4.5$. These results can be converted to any water depth D' by rescaling the time scales and velocities to $T' = rT$ and $U' = rU$ with $r = (D'/D)^{1/2}$. Theoretical solutions for irrotational and periodic waves over a flat bottom thus provide a variable maximum wave height as a function of the nondimensional depth kD which should correspond to the actual possible maximum height of periodic waves (Figure 2 (top)). It is expected that this theory can also provide some guidance for random waves, in particular in shallow water, where breakers take the form of quasi-solitary waves. There are certainly some differences between the idealized waves studied above and the real waves observed in the field, however we argue that there are also significant similarities that may justify the extension of this theory to irregular, rotational waves. Waves break when the crest orbital velocity u_c approaches or reaches the phase velocity C which leads to the crest overturning. We therefore believe that the crucial point in determining the breaking onset is the flow in the vicinity of the crest [*Longuet-Higgins*, 1973]. As stated above, Miche demonstrated that for regular, irrotational waves, the breaking criterion $u_c/C = 1$ was equivalent to $\beta/\beta_{\max} = 1$. By assessing $\beta/\beta_{\max}$ for our irregular waves we expect to obtain relevant information on the actual ratio u_c/C, a breaking parameter applicable for natural wind-generated waves in any water depth. Furthermore, *Dalrymple* [1974] successfully applied the approach detailed above to an irregular, asymmetric wave propagating over a linear shear current.

[13] Observations by *Thornton and Guza* [1983] have shown that broken waves in the surf zone may have a wide distribution of heights, related to $\tilde{\gamma}$. This parameter $\tilde{\gamma}$ also plays a dominant role in the wave energy dissipation parameterization by *Battjes and Janssen* [1978], in which the BWHD is defined as a delta function for the value $H = \tilde{\gamma}D$. Based on the empirical adjustment of this model to the observed energy of surf zone waves, *Ruessink et al.* [2003] proposed that $\tilde{\gamma}$ should vary with the peak normalized water depth k_pD, in the form

$$\tilde{\gamma} = 0.76k_pD + 0.29 \tag{3}$$

valid in the range $0.25 < k_pD < 0.7$.

[14] In *Ruessink et al.*'s [2003] and many other studies, the wave height measured is not a true wave height but rather it is $H_{rms,lin}$, a RMS wave height, estimated from the RMS bottom pressure time series using linear theory. Although the transformation from pressure to elevation poses no problem, the skewed shape of the wave profile generally gives different values for H_{rms} and $\sqrt{8m_0}$, with m_0 the surface elevation variance. If one processes monochromatic waves in the same manner, the actual wave height is strongly underestimated in shallow water due to the very sharp crest, which, for a wave of equal potential energy, can be twice as large as the height of an hypothetical linear wave given by the Airy theory. When one transforms the maximum wave height given by stream function theory to an equivalent linear wave height H_{lin} of equal potential energy, the maximum height scale appears close to the form given by *Ruessink et al.* [2003], for $kD < 0.3$ (Figure 2 (bottom)). For this situation it is possible to provide a polynomial fit to

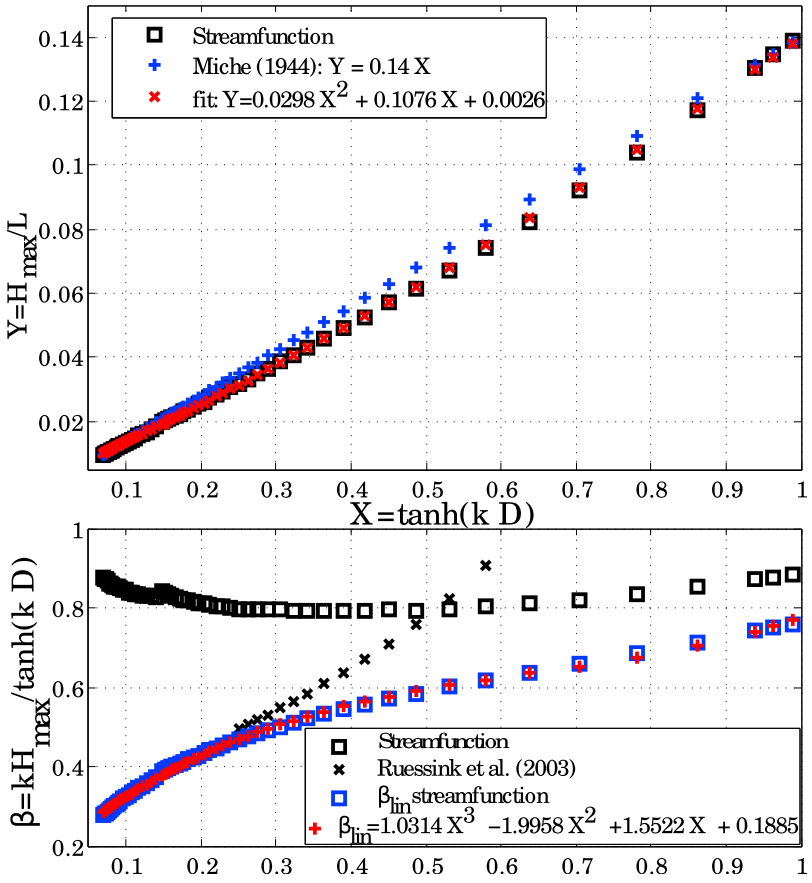

Figure 2. (top) The steepness of nearly breaking waves $Y = H_{max}/L$. The original breaking criterion of *Miche* [1944b] is recalled. A new criterion, using a second-order polynomial fit for H/L as a function of $X = \tanh(kD)$ is given. (bottom) The alternative nonlinearity parameter $\beta_{max,lin}$. In the case of *Ruessink et al.* [2003], the γ parameter is interpreted as H_{max}/D and transformed to $\beta_{max,lin}$, using the peak wave number k_p to estimate $\overline{k}$.

the maximal value of β as a function of $X = \tanh(kD)$ (see Figure 2 (bottom))

$$\beta_{max,lin} = 1.0314X^3 - 1.9958X^2 + 1.5522X + 0.1885. \quad (4)$$

However, for $0.3 \leq kD \leq 0.6$ the estimation of $\gamma_{RWS} = \tilde{\gamma}$ by *Ruessink et al.* [2003], corresponds to a β_{RWS} that is larger than that given by equation (4) (Figure 2). Because their analysis is based on a wave energy model that combines a breaking probability with a dissipation rate, either deep water waves may grow to larger heights than predicted by stream function theory, which appears unlikely, or β_{RWS} should be closer to $\beta_{max,lin}$, in which case the breaking dissipation rate is overestimated. Namely, a high bias in the model dissipation rate would cancel a low bias in the modeled breaking probability. Such a decreasing dissipation rate with increasing water depth, has been proposed by *Chawla and Kirby* [2002].

3. Breaking Probabilities of Dominant Waves in Various Environments

3.1. Data Set

[15] The data were collected during the AUSWEX (1997–2000) experiment in Lake George, Australia [e.g., *Babanin et al.*, 2001]. The wind and wave conditions observed during the experiment are reported in Table 1. The water was approximately 1 meter deep, as $k_pD \simeq 0.8$ the dominant waves were in finite depth. Besides, the waves were strongly forced. Two methods were employed to detect and quantify the breaking. *Babanin et al.* [2001] used spectrograms of recorded sound to identify the breaking occurrence, *Manasseh et al.* [2006] developed a method to detect bubble formation events along with the size of the bubbles formed. For each breaking event a brief pulse of sound was recorded and assumed to be that of a single freshly formed bubble. The bubbles radius was further inferred from the sound frequency, following Rayleigh-Plesset equation. Additionally, the breaking detection was visually verified.

3.2. Wave Scales Definition

[16] In section 3.4, we propose a parameterization of the BWHD in terms of the wave scales that we define here. *Banner et al.* [2000] and *Babanin et al.* [2001] assumed that the components contributing to the dominant waves (i.e., the waves whose frequency is approximately f_p) were contained between $(1 - \delta_{BBY})f_p$ and $(1 + \delta_{BBY})f_p$, with $\delta_{BBY} = 0.3$. *Manasseh et al.* [2006] reanalyzed the data set and found that the dominant breaking statistics observed by *Babanin et al.* [2001] were determined by the waves with $\delta' = 0.35$.

Table 1. Peak Frequency, Significant Wave Height, 10 Meter High Wind Speed, and Nondimensional Water Depth for Lake George Measurements[a]

Record	f_p (Hz)	H_s (m)	U_{10} (m/s)	k_pD
311823	0.36	0.45	19.8	0.82
311845	0.33	0.40	15.0	0.75
311908	0.35	0.37	12.9	0.72
311930	0.38	0.45	12.8	0.86
312021	0.40	0.39	13.7	0.92
312048	0.37	0.37	13.6	0.87

[a]Here f_p is the peak frequency, H_s is the significant wave height, U_{10} is the 10 meter high wind speed, and k_pD is the nondimensional water depth.

It is also interesting to remark that, for deep water waves, adopting such a frequency interval signifies that the dominant waves are formed from spectral components with wave numbers ranging from $0.5k_p$ to $1.7k_p$. The difficulty is to choose δ narrow enough in order to discriminate the energy of waves with different frequencies but also large enough so that the filtered surface has a steepness close to that of the original surface. *Banner et al.* [2000] also defined a representative wave height for the dominant waves

$$H_p = 4\sqrt{\int_{(1-\delta_{BBY})f_p}^{(1+\delta_{BBY})f_p} E(f)df}. \tag{5}$$

With $E(f)$ the energy spectrum of the waves. Here, we propose to extend this approach below and above the peak frequency to obtain a representative height, wave number and thus steepness of waves of different scales related to f_c

$$H_r(f_c) = \frac{4}{\sqrt{2}}\sqrt{\int_0^\infty U_{f_c}(f)E(f)df}. \tag{6}$$

The representative wave number corresponding to a given wave scale is defined as

$$\overline{k}_r(f_c) = \frac{\int_0^\infty U_{f_c}(f)k(f)E(f)df}{\int_0^\infty U_{f_c}(f)E(f)df}. \tag{7}$$

Where $U_{fc}(f)$ is a 2δ wide Hann window, centered at f_c (see Figure 3),

$$U_{f_c}(f) = 0.5 - 0.5\cos\left[\frac{\pi}{\delta}\left(\frac{f}{f_c} - 1 - \delta\right)\right]. \tag{8}$$

Compared to a rectangular window (as used in equation (5)) the Hann window does not modify much the result but is preferred because it reduces spectral leakage when going back to the time domain, as we do here. Because energy is lost, when filtering the spectrum with a Hann window instead of a rectangular window of the same width, we chose to broaden the Hann window by increasing the bandwidth δ up to 0.6 (Figure 3). For a JONSWAP spectrum and for the peak waves ($f_c = f_p$), this bandwidth gives the same energy as the $2\delta_{BBY}$ wide rectangular window. Because these windows are defined with a nondimensional width δ, the steepness $\overline{k}_r(f)H_r(f)$ is truly nondimensional and, thus, an appropriate measure of the wave geometry. Following *Phillips* [1958] and *Glazman* [1986], we assume that this geometry is closely related to breaking statistics. Obviously, wave directionality may also be important for breaking statistics. At present it is not clear whether the breaking probabilities, for a given wave scale, are isotropic or not [e.g., *Mironov and Dulov*, 2008]. The data used here do not, unfortunately, have directional information, and we shall leave the question of directionality for further studies.

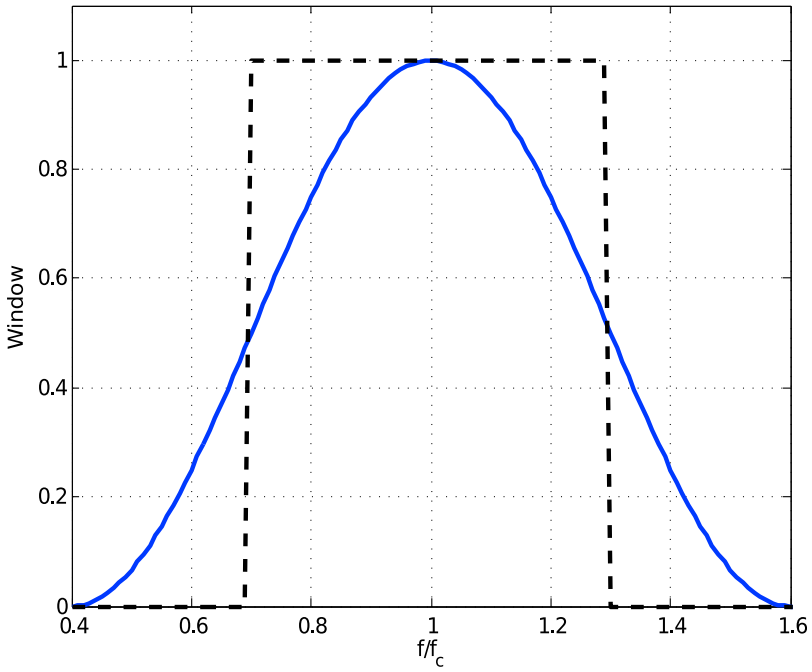

Figure 3. The Hann window given by equation (8), with δ = 0.6 (solid blue line), and rectangular window used by *Banner et al.* [2000] (dashed black line).

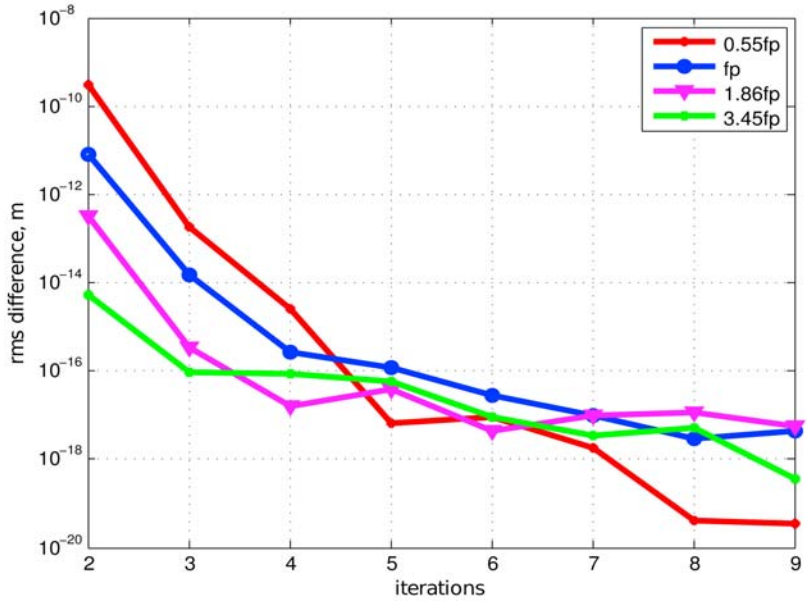

Figure 4. Root mean square deviation Δ_i^{fc} (equation (9)) shown for nine iterations and the four wave scales, processed from record 312048 (Lake George observations).

3.3. Data Analysis Method

[17] To associate a breaking event to a given wave scale, the classical method is the zero-crossing analysis, where the wave period is determined by the duration between two zero upcrossing of the elevation. In the current study, we develop a breaking probability suitable for the parameterization of the dissipation term in spectral models. In this context, waves are represented by a superposition of spectral components with several wave trains present at the same point and time, contrary to the zero-crossing decomposition. In the following, we shall first apply a spectral filter in order to discriminate different wave scales, and then apply the zero-crossing analysis.

3.3.1. Wave Scales Selection

[18] The spectrum is filtered with a Hann window (equation (8)) in order to select the spectral components contributing to the wave scales of interest. The waves of a given scale are first reconstructed in the time domain using the filtered spectrum. This approach is similar to a wavelet decomposition. The scales selected in this study are $0.55 \times f_p, f_p$, $1.86 \times f_p$ and $3.45 \times f_p$. With the Hann window (8), $\delta = 0.6$ gives only marginal overlap between the successive bandwidths. Moreover, since the waves contained in the bandwidth $3.45 f_p \pm \delta \times 3.45 f_p$ are approximately 1 meter long, and as shorter waves may not generate bubbles [*Longuet-Higgins*, 1986], we concluded that our method is not appropriate for higher frequencies, using acoustically determined breaking events.

3.3.2. Suppression of Nonlinear Contributions

[19] Because waves are not linear, this decomposition is artificial and each spectral bandwidth contains energy associated not only with linear waves but also with nonlinear harmonics belonging to other scales. As a consequence, the energy of the assumed linear waves may be overestimated. To remove the nonlinear contributions from the filtered signals, the amplitude of harmonics is estimated using the second-order theory by *Sharma and Dean* [1979].

[20] This processing is performed in several steps. First, for each scale, the high- and low-frequency harmonics are calculated and subtracted to the other scales. For example, we expect that the dominant scale may be contaminated by low- (respectively high) frequency harmonics of shorter (respectively longer) scales. The nonlinear contributions due to the other scales are filtered by the Hann window used for selecting the dominant scale before being subtracted to that scale. However, as the initial filtered waves contain nonlinear contributions, it is likely that the harmonics calculated are not exact. We endeavor to bypass this difficulty by repeating the process several times. The convergence of the results is displayed on Figure 4 for several iterations and shows a decrease of the RMS deviation between two successive iterations i and $i-1$ for the different wave scales f_c

$$\Delta_i^{f_c} = \frac{1}{N}\sqrt{\sum_{n=1}^{N}\left(s_{f_c}^{i}(t_n) - s_{f_c}^{i-1}(t_n)\right)^2}. \tag{9}$$

N is the length of the time series and $s_{f_c}^{i}$ is the filtered signal corresponding to the scale f_c at iteration i. Figure 4 suggests that the contribution of the second-order harmonics to the filtered signals is weak, and we further assume that higher-order nonlinearities can be neglected. An example of the filtering process is shown on Figure 5 where the initial and filtered waves are displayed as well as the sum of the filtered waves.

3.3.3. Breaking Events Assignment

[21] We now have a decomposition of the initial elevation time series over several wave scales. We further need to assign the breaking events to the right wave scale. For this,

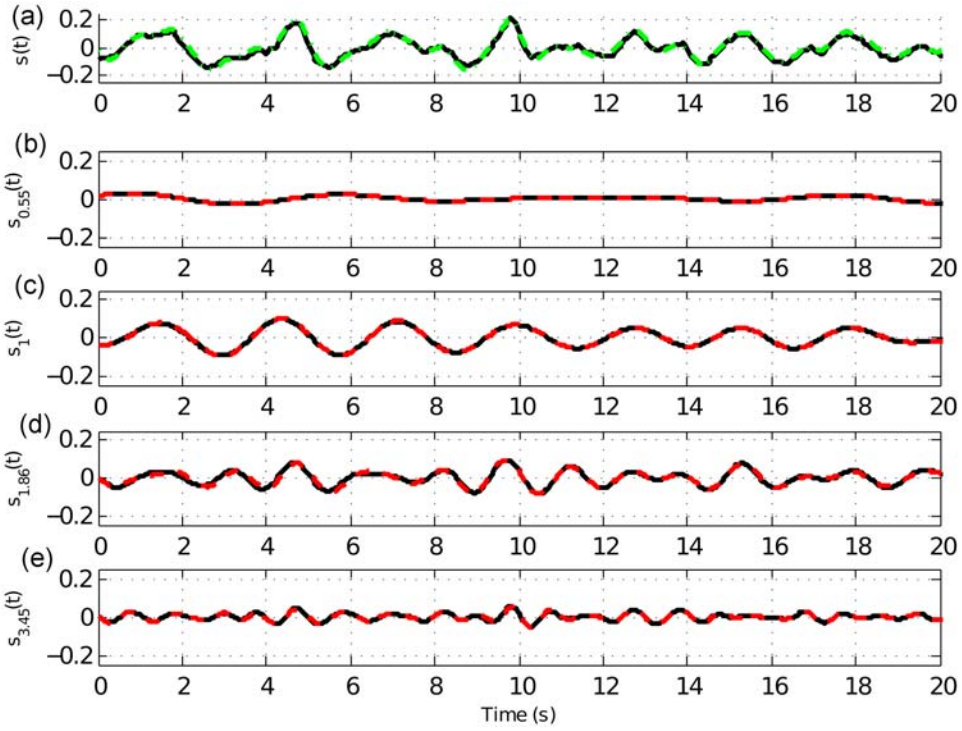

Figure 5. The 20 seconds of record 311930 filtered around the central frequencies (b) $f_c = 0.55f_p$, (c) f_p, (d) $1.86f_p$, and (e) $3.45f_p$ using a Hann window (black solid line), and the same signals corrected from nonlinearities (red dashed line), as described in section 3.3.2. (a) The original signal (solid black line) and the sum (dotted green line) of the filtered waves, corrected from nonlinearities $s_{0.55}(t)$, $s_1(t)$, $s_{1.86}(t)$, and $s_{3.45}(t)$. The height scale is in m.

each breaking event is assigned to a wave within each filtered signal. As our filtering analysis linearizes the waves, the harmonics that contributed to the sharp crests disappear which reduces the waves heights. Hence, $\beta/\beta_{\max,\mathrm{lin}}$ is assumed to provide guidance for detecting which of our filtered waves was more likely to be breaking. Therefore, $\beta/\beta_{\max,\mathrm{lin}}$ estimated from equations (2) and (4) is calculated for each wave, with k and H obtained from the zero up-crossing analysis of the filtered signal and the dispersion relationship. Finally, as shown in Figure 6, the breaking event is attributed to the wave with the largest $\beta/\beta_{\max,\mathrm{lin}}$.

[22] Because our method implies that only one wave is breaking at a given time, several ambiguous cases are likely to occur. First, the ratio $\beta/\beta_{\max,\mathrm{lin}}$ is estimated for waves that are already breaking, which implies that their heights may be already lower than just before breaking and that the breaking could be assigned to a steeper nonbreaking wave. Moreover, the breaking of large waves lasts a fraction of the wave period, therefore steep enough shorter waves riding in the vicinity of the large wave crest could, by mistake, be regarded as breaking waves. On the contrary, a short riding wave breaking on a longer wave could be missed if the longer wave parameter $\beta/\beta_{\max,\mathrm{lin}}$ is large enough. To reduce the number of such ambiguous situations, we impose that the breaking events located in the troughs of the peak waves cannot be assigned to those waves. Besides, two crossing wave trains may produce one single breaker and our approach is not able to deal with this situation, nor were the preexisting methods cited above.

3.4. Parameterization of the Breaking Wave Height Distribution

[23] The aim of the present paper is to provide a parameterization of the BWHD for different wave scales that will be used to build a dissipation source term for numerical wave forecasting models. The dissipation for the wave scale L is assumed to be the product of a BWHD times a dissipation rate, integrated over the distribution of wave heights [*Chawla and Kirby*, 2002]. This energy loss could then be distributed over the spectral wave components that form the waves of scale L. As the dissipation rate is expected to be a nonlinear function of wave height, possibly proportional to H^3 [*Chawla and Kirby*, 2002], it is necessary to have the BWHD, not just the breaking probability. *Thornton and Guza* [1983] investigated the BWHD in shallow water and introduced a parameterization $P_B(H)$ based on the Rayleigh distribution $P_R(H)$

$$P_B(H) = P_R(H) \times W(H). \tag{10}$$

Where $P_R(H)$ is

$$P_R(H) = \frac{2H}{H_{rms}^2} \exp\left(-\left(\frac{H}{H_{rms}}\right)^2\right). \tag{11}$$

Where H_{rms} is the root mean square wave height of the wave field. The weight function W transforms the height distribution of all the waves, P_R, into the height distribution of the breaking waves, P_B. According to *Thornton and Guza*

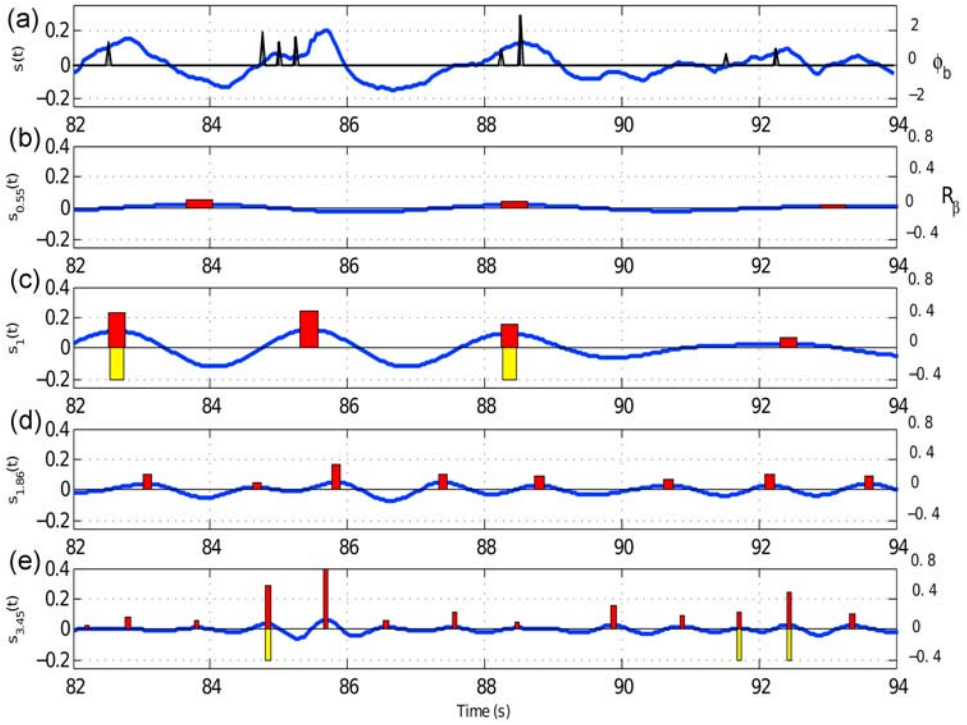

Figure 6. (top) The 12 second wave elevation for record 311908 in m (solid blue line, left axis) and bubbles radius Φ_b in mm (black spikes, right axis). (b–e) Filtered waves (solid blue line) and nonlinearity parameter $R_\beta = \beta/\beta_{\max,\mathrm{lin}}$ (red bars (upward), see right axis). The yellow bars (downward) indicate that the wave is breaking, the value was set arbitrarily at −0.4 for the sake of readability.

[1983], P_B should satisfy three conditions: it should fit the observations, it should be a subset of the distribution of all the waves, and $Q = \int_0^\infty P_B(H)dH$ should provide the breaking probability for the wave field. *Thornton and Guza* [1983] suggested

$$W_{TG}(H) = \left[\frac{\gamma_{rms}}{\tilde{\gamma}}\right]^2 \left\{1 - \exp\left[-\left(\frac{\gamma}{\tilde{\gamma}}\right)^2\right]\right\}. \quad (12)$$

Where

$$\gamma_{rms} = \frac{H_{rms}}{D}. \quad (13)$$

We propose to modify this formulation by introducing our wave scales and extending it to deep water

$$W_{FAB}(H, f_c) = a\left[\frac{\beta_r}{\tilde{\beta}}\right]^2 \left\{1 - \exp\left[-\left(\frac{\beta}{\tilde{\beta}}\right)^p\right]\right\}. \quad (14)$$

Here a and p are tunable parameters, $\tilde{\beta}$ is a linear function of $\beta_{\max,\mathrm{lin}}$ defined further, and

$$\beta_r = \frac{\bar{k}_r(f_c)H_r(f_c)}{\tanh(\bar{k}_r(f_c)D)}. \quad (15)$$

Moreover, the Rayleigh distribution for each wave scales is given by

$$P_R(H, f_c) = \frac{2H}{H_r^2(f_c)} \exp\left(-\left(\frac{H}{H_r(f_c)}\right)^2\right). \quad (16)$$

The form of W in equation (14) was initially used by *Chawla and Kirby* [2002] who investigated wave breaking over currents. They defined W with $H_r(f_c) = H_{rms}$, $\tilde{\beta} = 0.6$, $a = 1$ and $p = 2$. Their choice for W was motivated by the fact that it involves a Miche-type transition from deep to shallow water. Additionally, it tends to the breaking weight of *Thornton and Guza* [1983], that is known to agree with shallow water observations. However, as stressed by all authors, such a functional form for W is empirical, it is thus likely that other functions of $\beta/\beta_{\max,\mathrm{lin}}$ could also be appropriate for parameterizing W. Additionally, it is arguable that wave breaking may be affect by other physical processes such as the vertical shear of the surface current [*Papadimitrakis*, 2006]. Here we shall neglect such effects. For open ocean conditions, *Banner et al.* [2000] showed that involving the drift current into their parameterization did not significantly reduce the scatter of the observed breaking probabilities. This may be due to the fact that current shears are very weak in the open ocean [*Santala and Terray*, 1992; *Ardhuin et al.*, 2009].

[24] Here, we assume that $\tilde{\beta}$ is linearly related to the maximal value of β (corresponding to the breaking onset) found in section 2. Because filtering linearizes the waves, this yields

$$\tilde{\beta} = b \times \beta_{\max,\mathrm{lin}}. \quad (17)$$

Now we determine b, hence $\tilde{\beta}$, which constrains the shape of W_{FAB}. The parameter $\tilde{\beta}$ gives the inflexion point of W_{FAB}. Because *Thornton and Guza* [1983] did not filter the different wave scales, their analysis corresponds to the use of

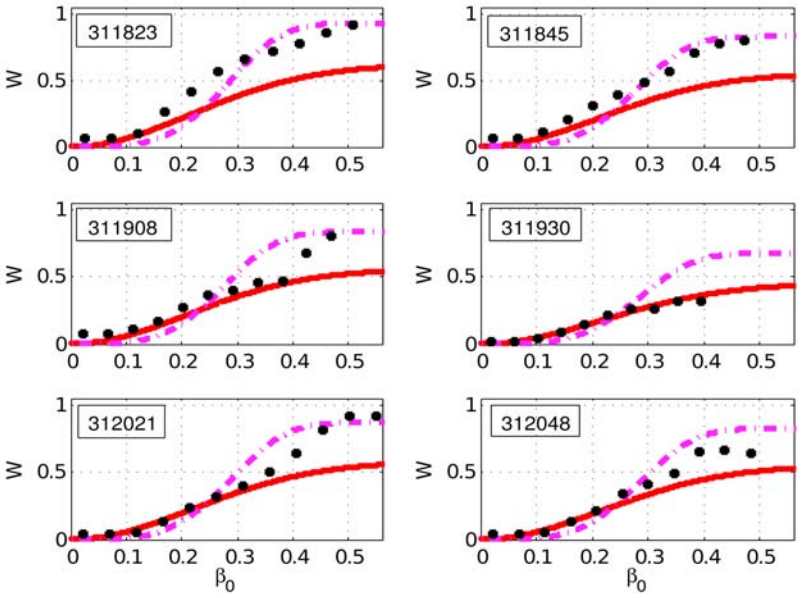

Figure 7. Breaking weights in terms of $\beta_0 = \overline{k}_r(f_p)H/tanh(\overline{k}_r(f_p)D)$ for the six Lake George records. Black circles are observed breaking weight, W_{obs}, solid red line is modeled breaking weight W_{FAB} with $a = 1$, $p = 2$, and dotted magenta line is W_{FAB} with $a = 1.5$, $p = 4$.

$\beta_{max} = 0.88$, the value given by Miche, instead of $\beta_{max,lin}$. From their observations, they found $b = 0.48$. We now determine empirically $\tilde{\beta}$, using the observations collected in Lake George. The behavior of $W_{obs} = P_{B,obs}/P_{R,obs}$ versus β, where $P_{B,obs}$ and $P_{R,obs}$ are the observed BWHD and wave height distribution is shown in Figure 7 for the peak waves. For this wave scale, the mean of $\beta_{max,lin}$ over the different records is 0.64. Figure 7 suggests $\tilde{\beta} \simeq 0.25$–$0.3$ for the peak waves, $b = 0.48$ is, thus, also consistent with Lake George observations.

[25] Once b is set, W_{FAB}, hence, P_{FAB} and Q_{FAB} are constrained by the free parameters a and p. As a is only a multiplicative constant, the shape of W_{FAB} is prescribed by p. Several values for p ($p = 2, 3, 4, 5$) were tested and for each p, a was chosen to best fit the Lake George observations, then, the corresponding parameterizations P_{FAB} and Q_{FAB} were investigated in deep and shallow water situations. However, only $p = 4$, $a = 1.5$ leads to satisfactory agreement with all the different data sets, especially with deep water observations. Besides, as $a = 1$ and $p = 2$ is the pair used by *Thornton and Guza* [1983] and *Chawla and Kirby* [2002], it is also interesting to examine its ability in diverse water depths. For the sake of clarity, only the results provided by $a = 1$, $p = 2$ and $a = 1.5$, $p = 4$ are shown in the paper. In the following, we explore the behavior of the BWHD, $P_{FAB}(H, f_c) = W_{FAB}(H, f_c)P_R(H, f_c)$, and of the breaking probability $Q_{FAB}(f_c) = \int_0^\infty P_{FAB}(H, f_c)dH$ versus breaking observations gathered in various water depths.

3.5. Investigations in Intermediate Water Conditions

[26] The parameterizations, P_{FAB} and Q_{FAB} are tested versus the breaking statistics of the different wave scales for the six records collected in Lake George. Figures 8 and 9 compare the observed and modeled breaking probability for the different wave scales and show a reasonable agreement with the data for the breaking probabilities. Deep water dominant breaking waves statistics are displayed on the same plot for the sake of completeness. These data were used by *Banner et al.* [2000] and gathered in the Black Sea and in the Southern Ocean. The description of these experiments are detailed by *Babanin et al.* [1993] (Black Sea observations) and *Banner et al.* [1999] (Southern Ocean data). Yet, as the dominant mean wave number $\overline{k}(f_p)$ were not available, we made the assumption that $\overline{k}(f_p) = 1.14f_p$, which is the value given by a JONSWAP spectrum [*Hasselmann et al.*, 1973], with an overshoot coefficient $\gamma_J = 1.7$. Overall, the agreement with the data is satisfactory, especially for the dominant scale. The short wave scales ($1.86\,f_p$ and $3.45\,f_p$) exhibit, however, a larger scatter. Especially, the shorter wave scale breaking probability is, in average, overestimated by our formulation. To explain this feature, one can advance that the scale $3.45\,f_p$ likely contains waves shorter than 1 meter long that are not supposed to produce bubbles while breaking. Our detection method is, thus, liable to miss some short wave-breaking events, which could result in an underestimation of the observed breaking probability, as shown on Figures 8 and 9. Additionally, Figures 10 and 11 display the modeled and observed BWHD for one of the Lake George record. For that particular record, Figure 10 supports that the formulation P_{FAB} with $a = 1.5$ and $p = 4$ provides the best fit to the data for the dominant scale. From Figure 11, one can conclude that the BWHD for the scale $0.55f_p$ is overestimated while using $a = 1$ and $p = 2$. Conversely, Figure 11 suggests that P_{FAB} with $a = 1.5$ and $p = 4$ generally underestimates the BWHD for the low heights. As said before, wave breaking may be influenced by a great number of other physical processes, that are not taken into account here. For instance, as Lake George waves are in finite water, there may exist a vertical shear current that may influence the breaking onset [*Banner*

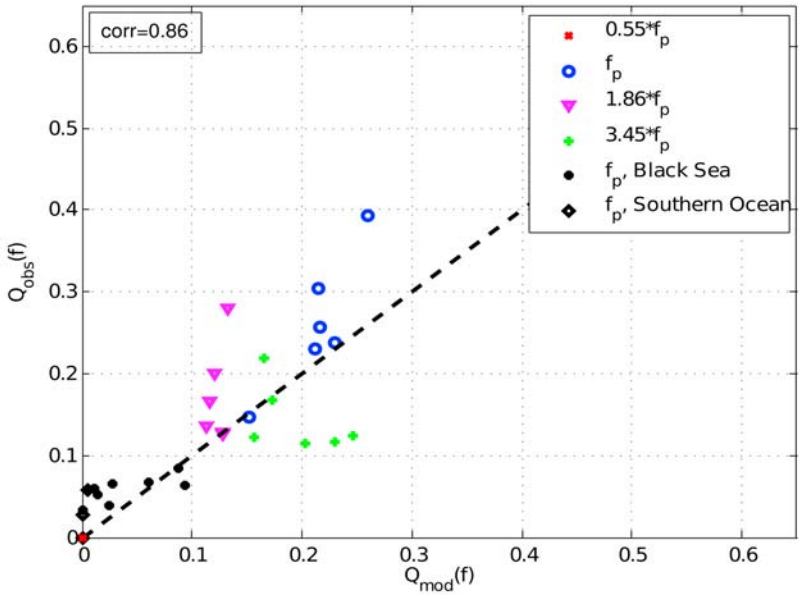

Figure 8. Modeled breaking probabilities $Q_{FAB}(f_c)$, with $a = 1$ and $p = 2$, compared to observed probabilities of several wave scales $Q_{obs}(f_c) = \int_0^\infty P_{B,obs}(H, f_c)dH$. The first four symbols (see legend) display the results for the four wave scales and the six Lake George records. The two last symbols represent the Black Sea and Southern Ocean data sets (dominant waves only) used by *Banner et al.* [2000].

and Phillips, 1974; *Papadimitrakis*, 2006], however, since no information on the current structure was available, we shall leave these issues for future studies. This section supports, nevertheless, that our formulations are capable of describing intermediate water breaking statistics, we, then, pursue our analysis by investigating their ability in deep water.

3.6. Validation in Deep Water Conditions

[27] Here, we propose to examine the ability of our formulation in deep water by comparing it to the parameterization derived by *Banner et al.* [2000] and to the data used in their paper. It is important to note that *Banner et al.* [2000] focused on the dominant waves, as a consequence we will not analyze the other scales. *Banner et al.* [2000] combined deep water data collected in various environments (Lake Washington, Black Sea and Southern Ocean) and reported that the breaking probability of the dominant waves exhibits a threshold behavior in terms of the spectral steepness $\epsilon = k_p H_p/2$. Namely, no dominant wave breaking was observed for ϵ less than 0.055. They proposed an empirical breaking

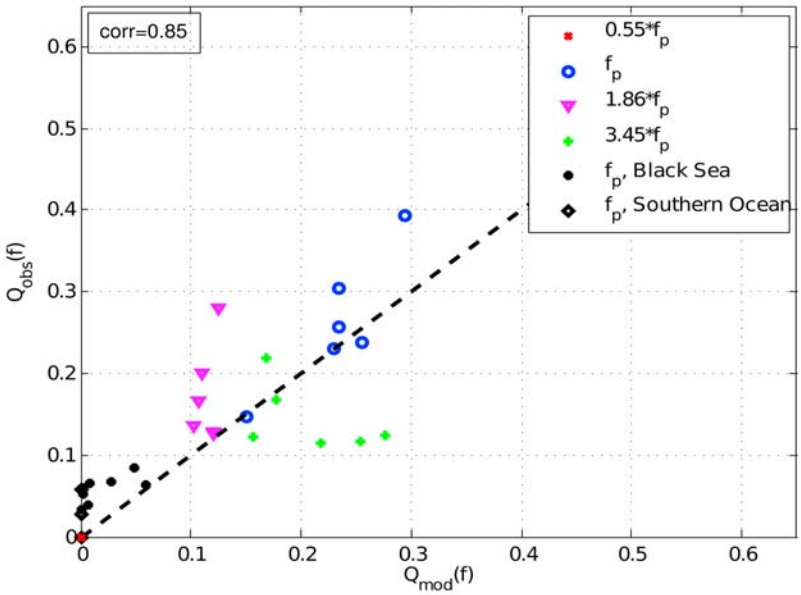

Figure 9. Same as Figure 8 except for $a = 1.5$ and $p = 4$.

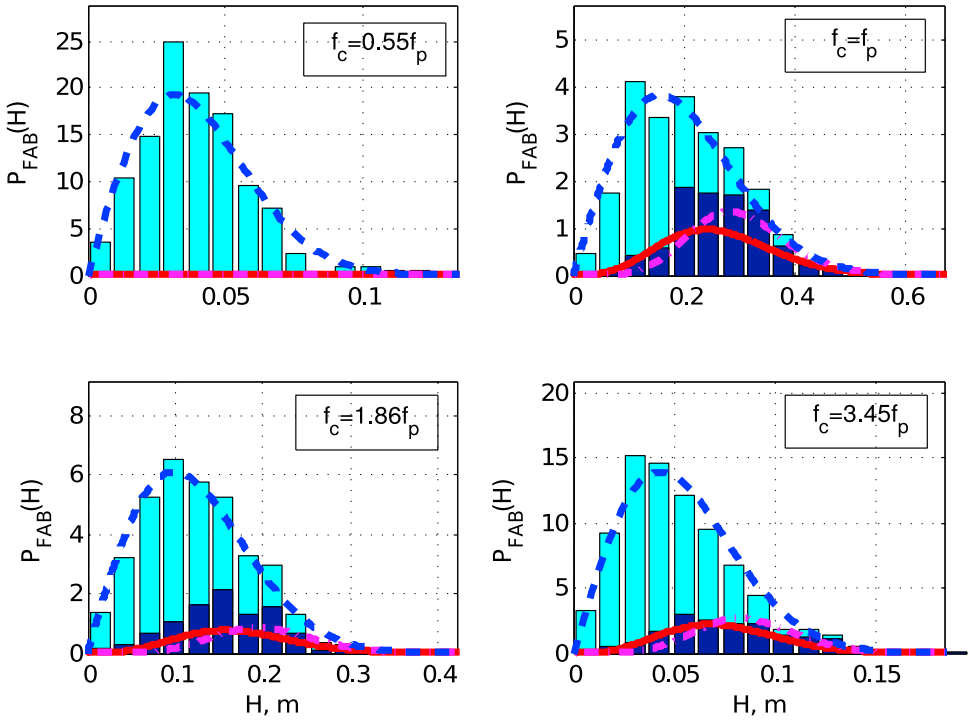

Figure 10. Observed wave height distribution (light blue bars, record 311823, Lake George data set); Rayleigh distribution (dashed blue line); observed BWHD (dark blue bars); modeled BWHD $P_{FAB}(H, f_p)$, with $a = 1$ and $p = 2$ (solid red line); and $P_{FAB}(H, f_p)$, with $a = 1.5$ and $p = 4$ (dotted magenta line). Each plot corresponds to a wave scale.

probability parameterization related to this behavior, which reasonably fit the three different data sets of observed breaking probabilities,

$$Q_{BBY}(f_p) \simeq 22(\epsilon - 0.055)^2. \quad (18)$$

Where $Q_{BBY}(f_p)$ is the breaking probability of the dominant waves. This approach can be generalized by introducing $\beta_r/\beta_{\max,\mathrm{lin}}$ instead of ϵ. In deep water, since $\beta_{\max,\mathrm{lin}}$ is constant, a breaking threshold on ϵ can readily be converted

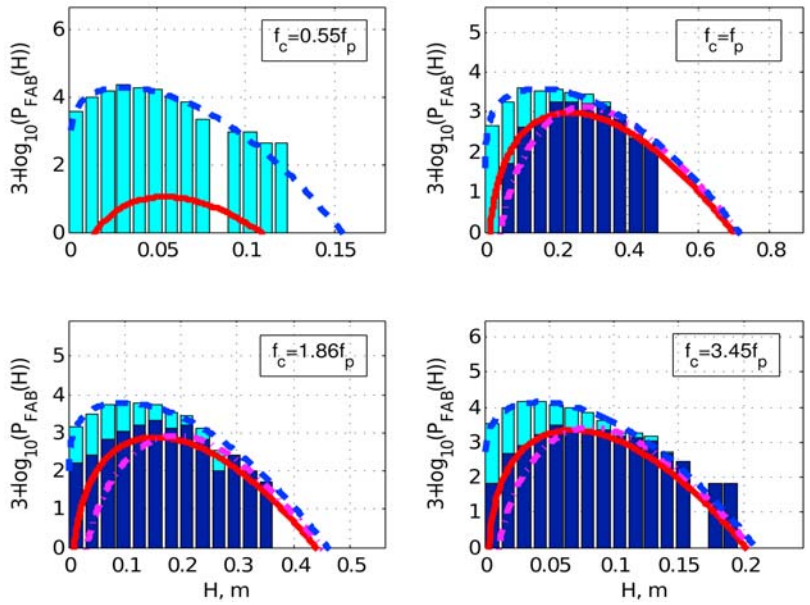

Figure 11. Same as Figure 10 but with vertical logarithmic scale.

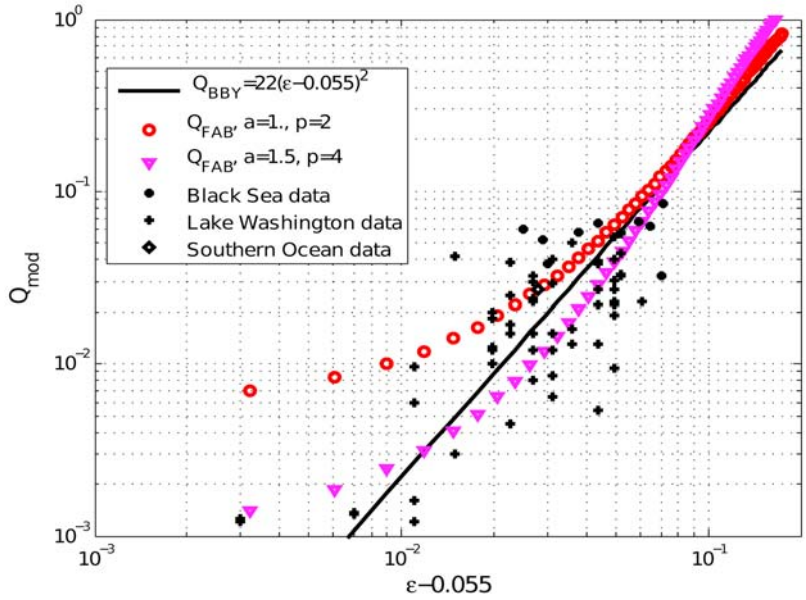

Figure 12. Comparison of the modeled breaking probabilities. Black solid line is $Q_{BBY}(f_p)$; red circles are $Q_{FAB}(f_p)$ with $a = 1$ ($a^* = 1.8$), $p = 2$; and magenta triangles are $a = 1.5$ ($a^* = 2.7$), $p = 4$. Additionally, observations reported by *Banner et al.* [2000] are displayed by black points for Black Sea data, black pluses for Lake Washington data, and black diamonds for Southern Ocean data.

into a breaking threshold on $\beta_r/\beta_{\max,\mathrm{lin}}$, where β_r is given by equation (15) with $f_c = f_p$. Namely,

$$Q_1(f_p) = 5(\beta_r/\beta_{\max,\mathrm{lin}} - 0.12)^2. \tag{19}$$

[28] Besides, because we need to define the BWHD, the most simple weighting function would be

$$W_1(H, f_p) = Q_1(f_p). \tag{20}$$

Since $\int_0^\infty P_R(H)dH = 1$, this approach is still consistent with the work of *Banner et al.* [2000], but as shown by Lake George observations (see Figure 7), a constant W is not a good approximation.

[29] We now examine how the breaking probability Q_{FAB} behaves in the conditions surveyed by *Banner et al.* [2000]. For this purpose, a JONSWAP spectrum, $E_J(f)$, was used, with $f_p = 0.125Hz$. The spectrum $E_J(f)$ was multiplied by an amplification factor, thus, providing a range of values for $\epsilon = k_p H_p/2$ corresponding to the observations of *Banner et al.* [2000]. However, the JONSWAP spectra approximation is an assumption that is important to keep in mind while analyzing further the results. Besides, as *Banner et al.* [2000] used a zero-crossing analysis to detect the waves, it is necessary to quantify the difference between the breaking probabilities measured in their study and those estimated in the present paper. We therefore explored the ratio $r_N = N_{filt}/N_{zc}$, where N_{zc} and N_{filt} are the number of dominant waves counted with the zero-crossing method and with the filtering analysis, respectively, presented in this paper. For the six records analyzed, the mean of r_N is

$$\bar{r}_N = 1.8 \tag{21}$$

and its standard deviation $\sigma_{r_N} = 0.05$. From this, we can estimate the difference in the breaking probabilities presented by *Banner et al.* [2000] with a zero-crossing analysis, and our filtering approach in which several waves can be superimposed at the same time. We thus correct our previous parameterizations, and a becomes $a^* = \bar{r}_N \times a$. For this particular case, the results are presented with $a^* = 1.8$, $p = 2$ and $a^* = 2.7$, $p = 4$. Figure 12 shows the comparison of our parameterization along with *Banner et al.* [2000] formulation and observations. The observations include the Black Sea and Southern Ocean data sets cited above, additionally, data from Lake Washington, described by *Katsaros and Ataktürk* [1992], are presented. Here, contrary to the intermediate water study the results vary significantly with p, and the combination ($a^* = 2.7$, $p = 4$) clearly provides the best fit to the data. The difference is particularly noticeable for low values of $\epsilon - 0.055$ where Q_{FAB} with $a^* = 1.8$, $p = 2$ largely overestimates the breaking probability. On the other hand, Q_{FAB} with $a^* = 2.7$, $p = 4$, is, on the whole, in acceptable agreement with observations. For $\epsilon - 0.055$ in the range [0.01–0.1], Q_{FAB} with $a^* = 2.7$, $p = 4$ is close to Q_{BBY}. Conversely, for $\epsilon - 0.055 > 0.1$ the gap between Q_{FAB} and Q_{BBY} increases significantly but no observations are available for deciding between Q_{BBY} and Q_{FAB}. For low dominant steepness ($\epsilon - 0.055 < 0.01$), a significant difference appears between Q_{BBY} and Q_{FAB}, and with ($a^* = 2.7$, $p = 4$), Q_{FAB} is in closer agreement with the data. Thus, our parameterization of the BWHD, with $a^* = 2.7$ and $p = 4$, produces dominant breaking probabilities that are also acceptable in deep water. We shall finally investigate the behavior of our parameterization in shallow water.

3.7. Validation in Shallow Water Conditions

[30] The W parameterization proposed in the present paper is mainly based on the formulation presented by *Thornton*

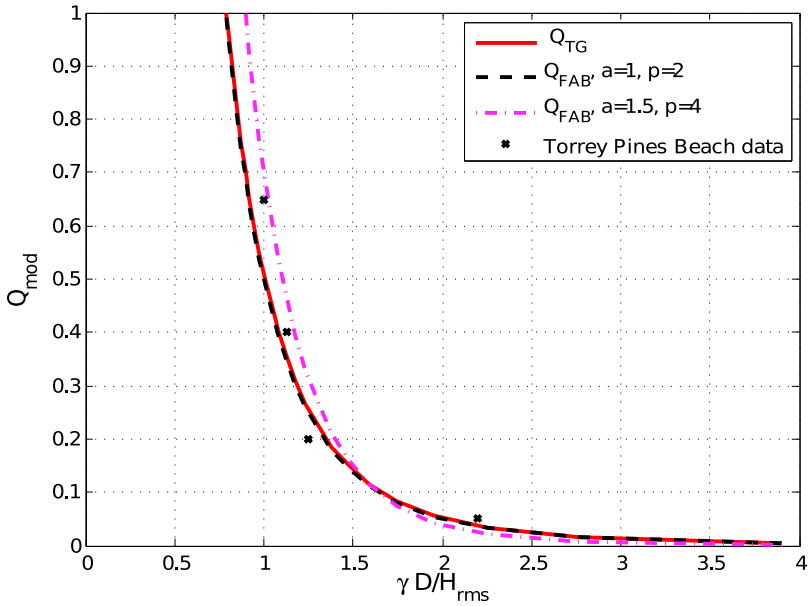

Figure 13. Q_{FAB} with $a = 1$ and $p = 2$ (solid red line) and with $a = 1.5$ and $p = 4$ (dotted magenta line) compared to Q_{TG} (dashed black line) and to observations presented by *Thornton and Guza* [1983] (black crosses).

and Guza [1983]. The major difference resides in the scale decomposition that was employed here for intermediate and deep water waves but which may be not relevant in shallow water. We will thus verify the influence of this modification.

[31] *Thornton and Guza* [1983] reported that they recorded low-frequency swell with negligible wind. Consequently, the frequency spectrum was probably narrow and following our formulation, the only existing wave scale might be the "dominant" one. Additionally, in these conditions, the wave heights detected by our analysis should not be underestimated, $\beta_{max,lin}$ must then be replaced by $\beta_{max} = 0.88$. This assumption implies that $b \times \beta_{max} = 0.42$ which is the value employed by *Thornton and Guza* [1983].

[32] In sections 3.5 and 3.6, we investigated the behavior of our breaking statistics parameterizations for $a = 1$, $p = 2$ and $a = 1.5$, $p = 4$. Although no significant difference was noted in intermediate water, the parameterization using $a = 1.5$, $p = 4$ was clearly more appropriate in deep water. The last step consists in examining the behavior of Q_{FAB} with $a = 1.5$, $p = 4$, in shallow water. For this, we used a narrow Gaussian spectrum, chosen such that the peak frequency bandwidth contains all the energy. The water depth and peak frequency were chosen in the range observed by *Thornton and Guza* [1983], typically, $d = 3.5$ m and $f_p = 0.075$ Hz. Along with the different parameterizations, Figure 13 displays observations gathered on Torrey Pines Beach, California (for more details, see *Thornton and Guza* [1982] or *Huntley et al.* [1981]). Figure 13 unsurprisingly suggests that Q_{FAB} with $a = 1$, $p = 2$ tends to *Thornton and Guza* [1983] breaking probability. It also appears that Q_{FAB} with $a = 1.5$, $p = 4$ is acceptable in shallow water. The three parameterizations are in close agreement with the data. The main difference between Q_{FAB} with ($a = 1.5$, $p = 4$) and the other formulations is its behavior for $\gamma D/H_{rms}$ close to unity, where it gives slightly higher values. These values are, however, consistent with the observations reported on Figure 13. In conclusion, under the assumptions given above, our approach is consistent with *Thornton and Guza* [1983] and with the available shallow water-breaking observations.

4. Discussion

[33] The aim of this study was to develop a parameterization able to predict the breaking statistics in all water depth conditions. Our analysis was guided by numerical results for irrotational monochromatic nearly breaking waves over a flat bottom. Additionally, an alternative method designed for measuring the breaking probabilities of waves of different scales has been introduced and discussed. The different wave scales are selected by means of a Fourier filtering. Besides, the spurious nonlinear contributions inherent to the Fourier analysis have been estimated and removed from the filtered signals using the second-order theory of *Sharma and Dean* [1979].

[34] Except for the nonlinear correction, our filtering method is similar to a wavelet analysis. We could have used other methods, such that the Riding Wave Removal method [*Schulz*, 2009] or the Empirical Mode Decomposition [*Huang et al.*, 1998]. However, this work has been used to build a dissipation term in a spectral wave model, that will be exposed elsewhere, and thus, the spectral analysis presented in the paper was found more appropriate.

[35] Clearly, the fact that a common parameterization of breaking wave height distributions (BWHD) may be used from shallow to deep water is an indication that all forms of wave breaking share some similarity, and that the breaking statistics may well be parameterized from a normalized filtered wave spectrum. This may be related to a dominance of the linear modulation of waves in the generation of unstable waves that evolve toward breaking. This relationship between spectra and breaking statistics is still not understood in detail. Ongoing work on the evolution of individual waves or wave

groups [e.g., *Banner and Tian*, 1998; *Babanin et al.*, 2007a], will likely shed some light on this question and eventually lead to more accurate parameterizations.

[36] The present work is still very empirical in nature, and many choices are relatively arbitrary. First, the dependence of the breaking weight W in terms of the nonlinearity parameter β, was chosen following the work done by *Thornton and Guza* [1983] and *Chawla and Kirby* [2002], who reported that this form was purely empirical. Other functions could then also be appropriate. Second, the wave scales selection relies on the width of the filtering window, which was empirically set. The window width could also depend, for instance, on the frequency and/or on the non-dimensional depth. In deep water, only the dominant waves have been studied, more data are then required to validate our formulation over the different wave scales that compose the wave field. Finally, wave breaking is likely affected by other parameters than the shape of the frequency spectrum. Among these, the directionality of the wave field and surface current shears may be relevant.

[37] The proposed breaking probability and BWHD formulations have been validated in intermediate water for different wave scales and in deep water for the dominant scale. In shallow water, our breaking statistics parameterization was shown to be similar to the one proposed by *Thornton and Guza* [1983] and consistent with data collected by the latter authors. Further acquisition of BWHD data in deep and intermediate water are planned and will be used to better constrain the functional shape of W_{FAB} and investigate the effects of other parameters. Our work supports that it is possible to obtain a unified parameterization for the breaking probabilities in all water depths. In particular it connects the shallow water breaking probabilities formulated in terms of wave height, to the deep water breaking probabilities formulated in terms of spectral saturation.

[38] **Acknowledgments.** We gratefully acknowledge contributions of the experimental group of the Australian Defence Force Academy, Canberra, Australian Capital Territory, Australia, who participated in collecting the original Lake George data set. A.V.B.'s research was partially supported by LP0883888 grant of the Australian Research Council and J.F.F. acknowledges the support of a CNRS-DGA doctoral research grant.

References

Ardhuin, F., T. H. C. Herbers, K. P. Watts, G. P. van Vledder, R. Jensen, and H. Graber (2007), Swell and slanting fetch effects on wind wave growth, *J. Phys. Oceanogr.*, *37*(4), 908–931, doi:10.1175/JPO3039.1.

Ardhuin, F., L. Marié, N. Rascle, P. Forget, and A. Roland (2009), Observation of Lagrangian, Stokes and Eulerian currents induced by wind and waves at the sea surface, *J. Phys. Oceanogr.*, *39*(11), 2820–2832.

Babanin, A., I. Young, and M. Banner (2001), Breaking probabilities for dominant surface waves on water of finite depth, *J. Geophys. Res.*, *106* (C6), 11,659–11,676.

Babanin, A., D. Chalikov, I. Young, and I. Savelyev (2007a), Predicting the breaking onset of surface water waves, *Geophys. Res. Lett.*, *34*, L07605, doi:10.1029/2006GL029135.

Babanin, A., R. Manasseh, I. Young, and E. Schultz (2007b), Spectral dissipation term for wave forecast models, experimental study, paper presented at 10th International Workshop on Wave Hindcasting and Forecasting and Coastal Hazards, Environ. Can., North Shore, Hawaii, 11–16 Nov.

Babanin, A. V., and I. R. Young (2005), Two-phase behaviour of the spectral dissipation of wind waves, paper presented at 5th International Symposium on Ocean Wave Measurement and Analysis, Am. Soc. of Civ. Eng., Madrid.

Babanin, A. V., P. Verkeev, B. Krivinskii, and V. Proshchenko (1993), Measurement of wind waves by mean of a buoy accelerometer wave gauge, *Phys. Oceanogr.*, *4*, 387–393.

Banner, M. L., and D. H. Peregrine (1993), Wave breaking in deep water, *Annu. Rev. Fluid Mech.*, *25*, 373–397.

Banner, M. L., and O. M. Phillips (1974), On the incipient breaking of small scale waves, *J. Fluid Mech.*, *65*, 647–656.

Banner, M. L., and X. Tian (1998), On the determination of the onset of breaking for modulating surface gravity water waves, *J. Fluid Mech.*, *367*, 107–137.

Banner, M. L., W. Chen, E. J. Walsh, J. B. Jensen, S. Lee, and C. Fandry (1999), The Southern Ocean Waves Experiment. Part I: Overview and mean results, *J. Phys. Oceanogr.*, *31*, 2130–2145.

Banner, M. L., A. V. Babanin, and I. R. Young (2000), Breaking probability for dominant waves on the sea surface, *J. Phys. Oceanogr.*, *30*, 3145–3160.

Banner, M. L., J. R. Gemmrich, and D. M. Farmer (2002), Multiscale measurement of ocean wave breaking probability, *J. Phys. Oceanogr.*, *32*, 3364–3374.

Battjes, J., and M. Stive (1985), Calibration and verification of a dissipation model for random breaking waves, *J. Geophys. Res.*, *90*(C5), 9159–9167.

Battjes, J. A., and J. P. F. M. Janssen (1978), Energy loss and set-up due to breaking of random waves, paper presented at 16th International Conference on Coastal Engineering, Am. Soc. of Civ. Eng., Hamburg, Germany.

Chawla, A., and J. T. Kirby (2002), Monochromatic and random wave breaking at blocking points, *J. Geophys. Res.*, *107*(C7), 3067, doi:10.1029/2001JC001042.

Cokelet, E. D. (1977), Steep gravity waves in water of arbitrary uniform depth, *Proc. R. Soc. London A*, *286*, 183–230.

Dalrymple, R. A. (1974), A finite amplitude wave on a linear shear current, *J. Geophys. Res.*, *79*, 4498–4504.

Dean, R. G. (1965), Stream function representation of nonlinear ocean waves, *J. Geophys. Res.*, *70*, 4561–4572.

Glazman, R. E. (1986), Statistical characterization of sea surface geometry for a wave slope field discontinuous in the mean square, *J. Geophys. Res.*, *91*(C5), 6629–6641.

Hasselmann, K., et al. (1973), Measurements of wind-wave growth and swell decay during the Joint North Sea Wave Project, *Dtsch. Hydrogr. Z.*, *8*(12), suppl. A, 1–95.

Huang, N. E., Z. Shen, S. R. Long, M. C. Wu, H. H. Shih, Q. Zheng, N.-C. Yen, C. Tung, and H. H. Liu (1998), The empirical mode decomposition and the Hilbert spectrum for nonlinear and non-stationary time series analysis, *Proc. R. Soc. London A*, *454*, 903–995.

Huntley, D. A., R. T. Guza, and E. B. Thornton (1981), Field observations of surf beat: 1. Progressive edge waves, *J. Geophys. Res.*, *86*(C7), 6451–6466.

Katsaros, K. B., and S. S. Ataktürk (1992), Dependence of wave-breaking statistics on wind stress and wave development, in *Breaking waves, 1991 IUTAM symposium Sydney, Australia*, edited by M. L. Banner and R. H. J. Grimshaw, pp. 119–132, Springer, Berlin.

Komen, G. J., K. Hasselmann, and S. Hasselmann (1984), On the existence of a fully developed windsea spectrum, *J. Phys. Oceanogr.*, *14*, 1271–1285.

Long, C. E., and D. T. Resio (2007), Wind wave spectral observations in Currituck Sound, North Carolina, *J. Geophys. Res.*, *112*, C05001, doi:10.1029/2006JC003835.

Longuet-Higgins, M. S. (1973), A model of flow separation at a free surface, *J. Fluid Mech.*, *57*, 129–148.

Longuet-Higgins, M. S. (1975), Integral relations of gravity waves of finite amplitude, *Proc. R. Soc. London A*, *342*, 157–174.

Longuet-Higgins, M. S. (1986), Acceleration in steep gravity waves. Part II: Subsurface accelerations, *J. Phys. Oceanogr.*, *16*, 1332–1337.

Manasseh, R., A. V. Babanin, C. Forbes, K. Rickards, I. Bobevski, and A. Ooi (2006), Passive acoustic determination of wave-breaking events and their severity across the spectrum, *J. Atmos. Ocean Technol.*, *23*, 599–618.

Miche, A. (1944a), Mouvements ondulatoires de la mer en profondeur croissante ou décroissante. Première partie. Mouvements ondulatoires périodiques et cylindriques en profondeur constante, *Ann. Ponts Chaussèes*, *114*, 42–78.

Miche, A. (1944b), Mouvements ondulatoires de la mer en profondeur croissante ou décroissante. Forme limite de la houle lors de son déferlement. Application aux digues maritimes. Troisième partie. Forme et propriétés des houles limites lors du déferlement. Croissance des vitesses vers la rive, *Ann. Ponts Chaussées*, *114*, 369–406.

Mironov, A. S., and V. A. Dulov (2008), Detection of wave breaking using sea surface video records, *Meas. Sci. Technol.*, *19*, 015405.1–015405.10, doi:10.1088/0957-0233/19/1/015405.

Papadimitrakis, Y. A. (2006), On the probability of wave breaking in deep waters, *Deep Sea Res. Part II*, *52*, 1246–1269.
Phillips, O. M. (1958), The equilibrium range in the spectrum of wind-generated waves, *J. Fluid Mech.*, *4*, 426–433.
Reul, N., and B. Chapron (2003), A model of sea-foam thickness distribution for passive microwave remote sensing applications, *J. Geophys. Res.*, *108*(C10), 3321, doi:10.1029/2003JC001887.
Ruessink, B. G., D. J. R. Walstra, and H. N. Southgate (2003), Calibration and verification of a parametric wave model on barred beaches, *Coastal Eng.*, *48*, 139–149.
Santala, M. J., and E. A. Terray (1992), A technique for making unbiased estimates of current shear from a wave-follower, *Deep Sea Res.*, *39*, 607–622.
Schulz, E. (2009), The riding wave removal technique: Recent developments, *J. Atmos. Ocean Technol.*, *26*, 135–144.
Sharma, J., and R. Dean (1979), Development and evaluation of a procedure for simulating a random directional second order sea surface and associated waves forces, *Ocean Eng. Rep. 20*, 112 pp., Univ. of Del., Newark, Del.
Stansell, P., and C. MacFarlane (2002), Experimental investigation of wave breaking criteria based on wave phase speeds, *J. Phys. Oceanogr.*, *32*, 1269–1283.
Tanaka, M. (1985), The stability of steep gravity waves. Part 2, *J. Fluid Mech.*, *156*, 281–289.
Thornton, E. B., and R. T. Guza (1982), Energy saturation and phase speeds measured on a natural beach, *J. Geophys. Res.*, *87*(C12), 9499–9508.
Thornton, E. B., and R. T. Guza (1983), Transformation of wave height distribution, *J. Geophys. Res.*, *88*(C10), 5925–5938.
van Vledder, G. P., and D. P. Hurdle (2002), Performance of formulations for whitecapping in wave prediction models, paper presented at 21st International Conference on Offshore Mechanics and Artic Engineering, Am. Soc. of Mech. Eng., Oslo, Norway, 23–28 June.
WISE Group (2007), Wave modelling—The state of the art, *Prog. Oceanogr.*, *75*, 603674, doi:10.1016/j.pocean.2007.05.005.
Wu, C. H., and H. M. Nepf (2002), Breaking criteria and energy losses for three-dimensional wave breaking, *J. Geophys. Res.*, *107*(C10), 3177, doi:10.1029/2001JC001077.
Young, I. R., and A. V. Babanin (2006), Spectral distribution of energy dissipation of wind-generated waves due to dominant wave breaking, *J. Phys. Oceanogr.*, *36*, 376–394.

F. Ardhuin and J.-F. Filipot, Service Hydrographique et Océanographique de la Marine, 13 Rue du Chatellier, F-29609 Brest, France. (ardhuin@shom.fr; jfilipot@shom.fr)

A. V. Babanin, Faculty of Engineering and Industrial Sciences, Swinburne University of Technology, Melbourne, Vic 3122, Australia. (ababanin@swin.edu.au)